Abnormalities in Glucose Uptake and Metabolism in Imatinib-Resistant Human BCR-ABL–Positive Cells

Douglas J. Kominsky,[1] Jelena Klawitter,[1] Jaimi L. Brown,[1] Laszlo G. Boros,[2] Junia V. Melo,[3] S. Gail Eckhardt,[4] and Natalie J. Serkova[1,4,5]

Abstract The development of imatinib resistance has become a significant therapeutic problem in which the etiology seems to be multifactorial and poorly understood. As of today, clinical criteria to predict the development of imatinib resistance in chronic myelogenous leukemia (CML), other than rebound of the myeloproliferation, are under development. However, there is evidence that the control of glucose-substrate flux is an important mechanism of the antiproliferative action of imatinib because imatinib-resistant gastrointestinal stromal KIT-positive tumors reveal highly elevated glucose uptake in radiologic images. We used nuclear magnetic resonance spectroscopy and gas chromatography mass spectrometry to assess ^{13}C glucose uptake and metabolism (glycolysis, TCA cycle, and nucleic acid ribose synthesis) during imatinib treatment in CML cell lines with different sensitivities to imatinib. Our results show that sensitive K562-s and LAMA84-s BCR-ABL–positive cells have decreased glucose uptake, decreased lactate production, and an improved oxidative TCA cycle following imatinib treatment. The resistant K562-r and LAMA84-r cells maintained a highly glycolytic metabolic phenotype with elevated glucose uptake and lactate production. In addition, oxidative synthesis of RNA ribose from ^{13}C-glucose via glucose-6-phosphate dehydrogenase was decreased, and RNA synthesis via the nonoxidative transketolase pathway was increased in imatinib-resistant cells. CML cells which exhibited a (oxidative/nonoxidative) flux ratio for nucleic acid ribose synthesis of >1 were sensitive to imatinib. The resistant K562-r and LAMA84-r exhibited a (oxidative/nonoxidative) flux ratio of <0.7. The changes in glucose uptake and metabolism were accompanied by intracellular translocation of GLUT-1 from the plasma membrane into the intracellular fraction in sensitive cells treated with imatinib, whereas GLUT-1 remained located at the plasma membrane in LAMA84-r and K562-r cells. The total protein load of GLUT-1 was unchanged among treated sensitive and resistant cell lines. In summary, elevated glucose uptake and nonoxidative glycolytic metabolic phenotype can be used as sensitive markers for early detection of imatinib resistance in BCR-ABL–positive cells.

Authors' Affiliations: [1]Department of Anesthesiology, University of Colorado Health Sciences Center, Denver, Colorado; [2]SiDMAP, LLC, Los Angeles, California; [3]Imperial College London, London, United Kingdom; and Departments of [4]Medicine and [5]Radiology, University of Colorado Denver, Anschutz Medical Center, Aurora, Colorado

Received 12/20/08; revised 1/22/09; accepted 2/10/09; published OnlineFirst 4/28/09.

Grant support: National Cancer Institute grants R21 CA108624 (N.J. Serkova, S.G. Eckhardt, J. Klawitter, D.J. Kominsky, and J.L. Brown) and P30CA046934 (N.J. Serkova, D.J. Kominsky, and J.L. Brown).

The costs of publication of this article were defrayed in part by the payment of page charges. This article must therefore be hereby marked *advertisement* in accordance with 18 U.S.C. Section 1734 solely to indicate this fact.

Note: D.J. Kominsky and J. Klawitter have contributed equally to this work.

Requests for reprints: Douglas J. Kominsky, University of Colorado Denver, Anschutz Medical Center, 12631 East 17th Avenue, MS 8202, Aurora, CO 80045. Phone: 303-724-7246; Fax: 303-724-1761; E-mail: Douglas.Kominsky@ucdenver.edu.

doi:10.1158/1078-0432.CCR-08-3291

Chronic myelogenous leukemia (CML) is a myeloproliferative disorder associated with a t(9;22) chromosomal translocation which gives rise to the Philadelphia chromosome, resulting in the production of a BCR-ABL fusion protein (1, 2). A large portion of a proto-oncogene on chromosome 9, called *ABL*, is translocated to the *BCR* gene on chromosome 22 (2). The two gene segments are fused and ultimately produce a chimeric protein that is larger than the normal ABL protein (3).

The development of novel targeted cancer-specific therapies is a major strategy in oncology, and the treatment of CML with imatinib mesylate (Gleevec or Glivec, formerly known as STI571) was the first successful proof of concept. Imatinib mesylate has revolutionized the way we treat CML its high level of activity, low toxicity, and ongoing durability have set a dramatic example by which future therapies in CML and cancer therapy overall will be judged. The therapeutic efficacy of imatinib is based on its specific inhibition of the BCR-ABL tyrosine kinase

Translational Relevance

The metabolic signature of imatinib resistance can reliably reveal therapeutic sensitivity to imatinib treatment. This can be readily evaluated by nuclear magnetic resonance in chronic myelogenous leukemia (CML) cell lines as well as applied to assess glucose metabolism in leukocytes isolated from patients with imatinib-treated CML, using the same approach as described in the present study with clonal cell lines. In future clinical studies, we will test whether the metabolic effect [increased glucose uptake with elevated (glycolysis/TCA) ratios] can be detected in the "to-be-resistant" cells prior to an increase in the white cell count. If validated, the glucose assessment can help (*a*) to develop a clinical magnetic resonance spectroscopy–based metabolic profile in peripheral blood for the early detection of imatinib resistance in patients with CML, and (*b*) to evaluate the metabolic mechanisms of action for novel small molecule tyrosine kinase inhibitors. In addition, metabolic enzyme inhibitors may be tested as possible therapeutic alternatives for imatinib-resistant cells.

at the ATP-binding site of the Abl moiety, which results in significant improvement of the outcome in CML (4, 5).

Unfortunately, responses to imatinib in patients with advanced CML are often transient, generally lasting less than 6 months (6, 7). Furthermore, the emerging problem of resistance (even in chronic-phase CML) limits the long-term treatment benefit of imatinib; in accelerated and blastic-phase disease, 51% and 88% of patients, respectively, will relapse after 24 months of imatinib treatment. The development of imatinib resistance has become a major therapeutic problem (6, 8), and can be due to point mutations in the Abl kinase domain, *BCR-ABL* gene amplification at the genomic or transcript level and overexpression, activation of other tyrosine kinases such as the Scr-related LYN kinase, overexpression of multidrug-resistant proteins such as P-gp, and variability in the amount and function of the drug influx protein OCT-1 (9–15).

Clinical criteria to predict the development of imatinib resistance in CML, other than rebound of myeloproliferation, are currently under development. However, it has been shown that *BCR-ABL*–positive cells express high-affinity GLUT-1 glucose transporter and have increased glucose uptake (16, 17). When exposed to imatinib, the responsive cells have decreased glucose uptake and lactate production (18), and restricted use of glucose carbons for *de novo* fatty acid synthesis (19, 20). One of the reasons for the reduced hexose uptake activity is caused by a redistribution of glucose transporters from the cell membrane to the interior (21).

Imatinib-resistant gastrointestinal stromal KIT–positive tumors reveal highly elevated glucose uptake in the primary tumor as well as in brain metastatic lesions in clinical positron emission tomography scans (22, 23). Moreover, an improvement in fasting glucose in patients with CML and type 2 diabetes mellitus treated with imatinib, was reported, allowing for a reduction in insulin or glucose-lowering drugs (24, 25).

Currently, there is no information about the changes in cell glucose metabolism during imatinib resistance development in patients with CML. Therefore, the early detection of therapeutic responsiveness by associated metabolic profiles in CML cells will provide clinical benefit from early intervention. We hypothesize that human *BCR-ABL*–positive leukemia cells with acquired resistance to imatinib will express a distinctively different glucose uptake and glucose metabolism when compared with imatinib-treated sensitive cells. The goal of this study was to elucidate the molecular mechanisms underlying glucose transport and the metabolic phenotype of imatinib-resistant cells. We used nuclear magnetic resonance (NMR) spectroscopy and gas chromatography mass spectrometry (GC-MS) approaches for stable ^{13}C isotope–based metabolic profiling to explore the effects of imatinib treatment in CML cell lines with different sensitivities to imatinib. We correlated ^{13}C-glucose uptake and metabolism with intracellular expression and localization of GLUT-1 transporter protein in these cells.

Materials and Methods

Cell cultures and imatinib treatment. Two imatinib-sensitive CML cell lines, K562-s and LAMA84-s, as well as their resistant counterparts K562-r and LAMA84-r (resistant to 1 μmol/L imatinib) were generated in the laboratory of Dr. Melo as previously described (26). Decreased inhibition of *BCR-ABL* autophosphorylation in K562-r cells, and upregulation of *BCR-ABL* and MDR1 p-glycoprotein in LAMA84-r cells were discussed as their possible mechanisms of resistance to imatinib (26). All cells were grown in RPMI 1640 culture medium containing 10% fetal bovine serum (both from Invitrogen, Co.). The cells were kept at 37°C with 95% air/5% CO_2. Imatinib was kindly provided by Dr. E. Buchdunger (Novartis Pharmaceuticals, Basel, Switzerland). The sensitive K562-s and LAMA84-s cells were treated with 1 μmol/L of imatinib for 24 h. The resistant cells were constantly grown in the presence of 1 μmol/L of imatinib. Cell proliferation and viability were examined by cell counting using a cell counter (Beckman) and trypan blue exclusion, respectively.

Western blots for GLUT-1 protein expression. Cells were pelleted by centrifugation, washed with ice-cold PBS, and lysed by sonication in 150 μL of radioimmunoprecipitation assay buffer [50 mmol/L Tris-HCl (pH 7.4), 150 mmol/L NaCl, 2 mmol/L EDTA, 1% NP40, and 0.1% SDS], and protease inhibitors (complete cocktail tablets; Roche Applied Science). Protein concentration was assessed by the bicinchoninic acid assay following the manufacturer's instructions (Pierce Biotechnology) in order to ensure equal protein loading of each preparation. Proteins were separated by SDS-PAGE electrophoresis and transferred to nitrocellulose membrane (Bio-Rad Laboratories) for immunoblotting. Blots were probed with the anti–GLUT-1 antibody (DakoCytomation) at a dilution of 1:200 and anti-actin antibody (Sigma-Aldrich) at a dilution of 1:50,000. Proteins were visualized using the SuperSignal detection substrate (Pierce Biotechnology).

Reverse transcription-PCR for GLUT-1 protein expression. RNA was extracted using the RNeasy Mini Kit (Qiagen) and quantified by UV spectrometry at 260 nm. The integrity of the RNA preparation was determined using an Agilent Bioanalyzer (model 2100). Real-time PCR was done using QuantiTect SYBR-Green RT-PCR Kit (Qiagen). Relative quantification of GLUT-1 expression was determined by comparison of the amount of GLUT-1 transcript to the housekeeping gene glyceraldehyde-3-phosphate dehydrogenase (GAPDH). The following primer sets were used: GLUT-1 forward sequence, ACC CTG GAT GTC CTA TCT GAG C; GLUT-1 reverse sequence, GCT GAA GAG TTC AGC CAC GAT; GAPDH forward sequence, CAG CCT CAA GAT CAT CAG CAA; GAPDH reverse sequence, GGT CAT GAG TCC TTC CAC GAT AC. Reactions were run in triplicate,

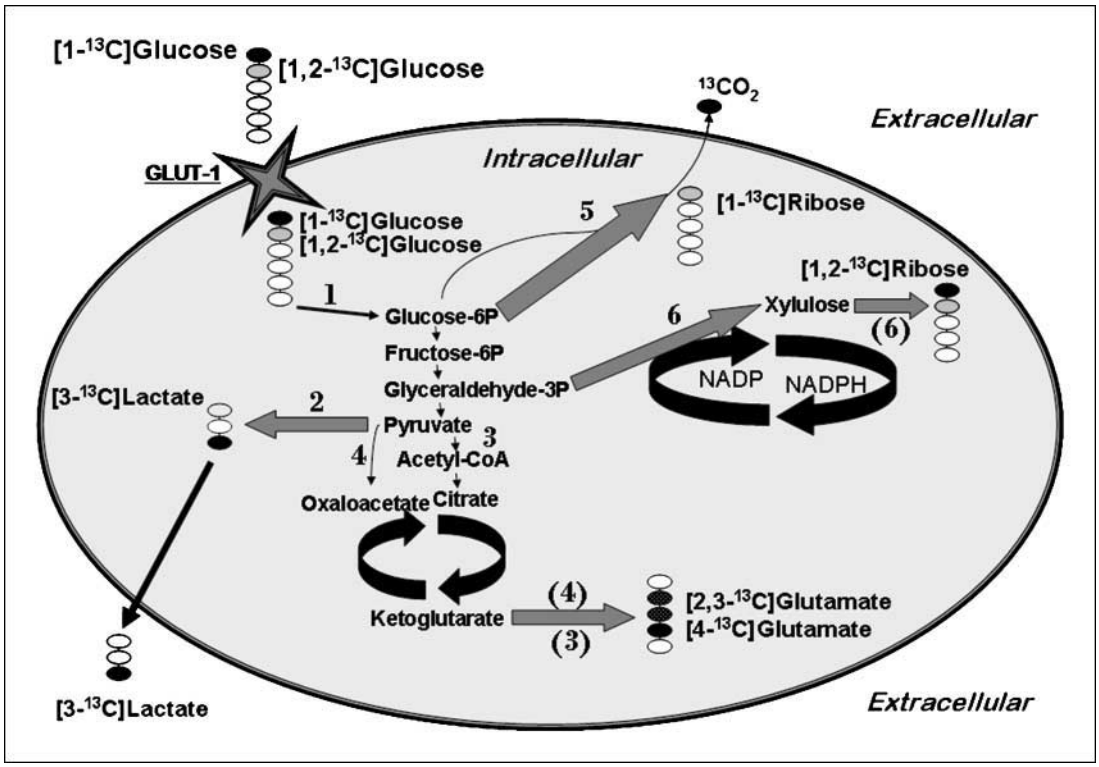

Fig. 1. Metabolic chart of ^{13}C carbon enrichment through glycolysis, the TCA cycle, and the pentose phosphate pathway after incubation with ^{13}C-glucose as a labeled precursor (either [1-^{13}C] or [1,2-^{13}C]glucose). After glucose is transported into the cells (GLUT-1 transporter protein for leukemia cells), it is phosphorylated by a hexokinase to form glucose 6-phosphate (*Glucose-6P*). Glucose 6-phosphate can then enter a number of metabolic pathways with glycolysis, the TCA cycle and the pentose phosphate pathway being the most important for the leukocytes.

and three independent experiments were run for each sample. Comparison of gene expression in a semiquantitative manner was done based on the mathematical model of Pfaffl (27).

2-Deoxy-D-glucose uptake assay. Imatinib-resistant and imatinib-sensitive cells (1×10^7 cells/mL) treated with 1 μmol/L of imatinib for 24 h were pelleted, washed twice with PBS, and quickly fixed with freshly prepared 4% paraformaldehyde in PBS (dilution of 30% formaldehyde stock in PBS) for 20 min at room temperature. The cell suspension was washed five times with PBS. Cells were permeabilized with cold acetone for 7 min at −20°C, followed by three washes with PBS. Cells were incubated in blocking buffer (10% fetal bovine serum, 0.1% Triton X-100 in PBS) for 1 h at room temperature. For GLUT-1 localization studies, cells were incubated for 2 h with blocking buffer containing anti–Glut-1 antibody (DakoCytomation) at a dilution of 1:200. Control cells were incubated with anti-CD33 antibody (Santa Cruz Biotechnology) at a 1:100 dilution as a control for surface membrane staining. Cells were washed four times with 0.1% Triton X-100 in PBS, then incubated with a FITC-labeled anti-rabbit secondary antibody (Amersham Biosciences) at a 1:20 dilution. The incubations were done at room temperature in the dark for 1 h. Prior to imaging, cells were washed thrice with 0.1% Triton X-100 in PBS, once with PBS, and finally with distilled water. Microscopy was done using a Digital Deconvolution microscopy imaging system based on a Zeiss Axioplan 2 Epifluorescence upright microscope platform. All images were digitally captured with a Cooke Sensicam QE high resolution (1,376 × 1,024 resolution) black and white supercooled CCD camera.

2-Deoxy-D-glucose uptake assay. Cells in mid-log phase (1×10^7 cells/mL) were used for the hexose uptake assay as described elsewhere (21). The sensitive cells were treated with 0.1 or 1 μmol/L of imatinib for 24 h. The resistant cells were kept constantly in the presence of 1 μmol/L of imatinib. The cells were washed twice with PBS to remove glucose. The cells were resuspended in 100 μL of PBS supplemented with 5 mmol/L of 2-deoxy-D-glucose (containing 2 μCi/mL 2-deoxy-[1-^3H]glucose; refs. 21, 28) and incubated at 37°C for 5, 10, 20, 30, 40, 50, and 60 min. The uptake was stopped by the addition of 100 μL of ice-cold PBS with 100 μmol/L of phlorentin. The cells were transferred to 1.5 mL reaction tubes and centrifuged at 20,000 × *g* for 30 s. Cell pellets were washed once and put into a scintillation vial containing 10 mL of Optifluor (Perkin-Elmer, Inc.). The incorporated radioactivity was measured by a liquid scintillation counter (Perkin-Elmer). The intracellular concentrations of 2-deoxy-[1-^3H]glucose were reported as nmol/10^4 cells.

[1-^{13}C]-glucose uptake and metabolism studies by multinuclear magnetic resonance spectroscopy. By the end of 24 h of imatinib treatment, the cells were incubated with 5 mmol/L of [1-^{13}C]glucose (Cambridge Isotope Laboratories) for 4 h before perchloric acid extraction. All cell extractions were done using a previously published perchloric acid extraction protocol (18). Lyophilized medium and water-soluble cell extracts were redissolved in 0.5 mL of deuterium oxide, respectively. After centrifugation, the supernatants were neutralized (to pH 7.2) to allow precise chemical shift assignments. High-resolution ^1H- and ^{13}C-NMR experiments were done with the Bruker 500 MHz DRX spectrometer equipped with an inverse 5 mm TXI probe (Bruker BioSpin). For proton NMR, a standard water presaturation pulse program was used for water suppression. Trimethylsilyl propionic-2,2,3,3,-d_4 acid (0.5 mmol/L) was used as an external standard for metabolite chemical shift assignment (0 ppm) and quantification. ^{13}C-NMR spectra with proton decoupling were recorded using the C3-lactate peak at 21 ppm as chemical shift reference and for quantification of ^{13}C spectra. Extracellular concentrations of [1-^{13}C]glucose and of exported [3-^{13}C]lactate were calculated in the medium. [1-^{13}C]Glucose uptake was calculated as the difference between initial glucose concentrations (5 mmol/L) and detected extracellular glucose levels in the medium after incubation. In the cell extracts, intracellular [1-^{13}C]glucose and its ^{13}C-labeled

intermediates from glycolysis, [3-^{13}C]lactate, as well as from the TCA cycle, [4-^{13}C]glutamate, were calculated from ^{13}C-NMR spectra. All NMR spectra were processed using the Bruker WINNMR program.

[1,2-^{13}C]Glucose metabolism by GC-MS. For GC-MS analysis on nucleic acid synthesis, the cells were incubated with imatinib and 5 mmol/L of [1,2-^{13}C]glucose for 60 h and extracted as previously reported (29). Mass spectral data were obtained on the Agilent 5973 Network mass selective detector connected to the Agilent 6890 Network GC system. The GC-MS settings were GC inlet 250°C, transfer line 280°C, MS source 230°C, and MS Quad 150°C. An HP-5 capillary column (30 m length, 250 μm diameter, 0.25 μm film thickness) was used for glucose, ribose, and deoxyribose ^{13}C-MS analysis. The representative carbon fluxes from [1,2-^{13}C]glucose through the oxidative branch of the pentose cycle, [1-^{13}C]ribose and [1-^{13}C]deoxyribose, and through the nonoxidative branch, [1,2-^{13}C]ribose and [1,2-^{13}C]deoxyribose, are presented in Fig. 1.

Statistical analyses. All experiments were repeated at least four times. All numerical data are presented as mean ± SD. The ANOVA method was used to determine differences between groups (untreated sensitive versus treated sensitive versus resistant). The significance level was set at $P < 0.05$ for all tests (SigmaPlot-version 9.01, Systat Software).

Results

Glucose uptake and metabolism in imatinib-sensitive and imatinib-resistant cells. In this study, we have combined two novel metabolomics profiling techniques, NMR and GC-MS, to globally assess ^{13}C-glucose fluxes. Figure 1 illustrates the metabolic fate of ^{13}C carbon through glycolysis, the TCA cycle, and the pentose phosphate pathway after incubation with ^{13}C-glucose as a labeled precursor, as detected through the combination of the abovementioned techniques.

In both cell lines, K562-s and LAMA84-s, treatment with 1 μmol/L of imatinib for 24 hours significantly reduced glucose uptake and lactate export (Table 1; Fig. 2). Additionally, decreased concentrations of [4-^{13}C]glutamate were observed, indicating a reduction in the cytosolic glycolysis as well as the mitochondrial TCA cycle activity (Table 1; Fig. 2).

Interestingly, imatinib-resistant LAMA84-r and K562-r cells maintained in 1 μmol/L of imatinib showed slightly different profiles regarding their glucose utilization patterns. Both cell lines exhibited significantly higher levels of glucose uptake and lactate export compared with both sensitive control and sensitive exposed cells (Table 1; Fig. 2). These results indicate that the imatinib-resistant cells exhibit a highly glycolytic phenotype.

As an alternative approach to monitoring glucose uptake in CML cell lines, we used a 2-deoxy-D-glucose uptake assay. The sensitive cells were treated with 0.1 or 1 μmol/L of imatinib for 1 and 24 hours. The resistant cells were kept constantly in the presence of 1 μmol/L of imatinib. The incorporated radioactivity was measured and intracellular concentrations of 2-deoxy-[1-^{3}H]glucose are shown in Fig. 3. These results confirm our ^{13}C-NMR data and show that imatinib-sensitive cells (both K562-s and LAMA84-s) exhibit reduced glucose uptake and that this reduction is time-dependent and concentration-dependent. In contrast, resistant K562-r and LAMA84-r cell lines displayed higher glucose uptake than their sensitive counterparts (Fig. 3). This suggests that the ability to import and utilize glucose is an important consequence of imatinib resistance development.

Nucleic acid ribose synthesis after the addition of [1,2-^{13}C] glucose. All human cells, including CML cells, possess two major pathways to produce nucleic acid precursors: (*a*) the oxidative and (*b*) the nonoxidative route of the pentose cycle (Fig. 1). Utilization of [1,2-^{13}C]glucose through the oxidative pathway results in the production of RNA [1-^{13}C]ribose or DNA [1-^{13}C] deoxyribose via glucose-6-phosphate dehydrogenase (G6PDH). The nonoxidative glucose pathway results in the production of RNA [1,2-^{13}C]ribose and DNA [1,2-^{13}C]deoxyribose via transketolase activity. The resistant K562-r and LAMA84-r showed a unique and significantly altered ratio of ribose synthesis in the pentose cycle. As shown in Fig. 4A, oxidative synthesis of ribose via G6PDH was decreased and glucose flux via the nonoxidative transketolase pathway was increased. CML cells that exhibited an oxidative/nonoxidative flux ratio for nucleic acid ribose synthesis of 1 or higher were sensitive to imatinib. The resistant K562-r and LAMA84-r exhibited a (oxidative/nonoxidative) flux ratio of <0.7. Similarly, oxidative synthesis of deoxyribose through the G6PDH pathway was decreased and synthesis via the transketolase pathway was increased, although not significantly (Fig. 4B).

Alteration of GLUT-1 localization in imatinib-sensitive and imatinib-resistant cells. After showing that alteration in glucose uptake and utilization occurred in imatinib-resistant cells, we did experiments to determine transport mechanisms underlying this phenotypic change. To that end, we used digital deconvolution microscopy to examine the localization of GLUT-1, the major glucose transport protein in leukocytes. As shown in Fig. 5A, GLUT-1 is localized to the plasma membrane of untreated K562-s cells, exhibiting uniform staining around the cell periphery. Conversely, in K562-s cells treated for 24 hours with 1 μmol/L of imatinib, GLUT-1 staining is quite dif-

Table 1. Intracellular and extracellular concentrations of ^{13}C-labeled metabolites (μmol/g cell weight) from [1-^{13}C]glucose in LAMA84 and K562 cell extracts as calculated from ^{13}C-NMR spectra

	[1-^{13}C]glucose uptake	[3-^{13}C]lactate export (extracellular)	[3-^{13}C]lactate intracellular	[4-^{13}C]glutamate intracellular
LAMA84-s untreated	914.14 ± 86.52	82.52 ± 14.03	2.38 ± 0.66	0.25 ± 0.05
LAMA84-s +1 μmol/L (24 h)	711.84 ± 104.06**	60.07 ± 11.81**	1.73 ± 1.04*	0.16 ± 0.03*
LAMA84-r (1μmol/L)	1,049.55 ± 112.31*	117.86 ± 13.44***	4.11 ± 2.19***	0.36 ± 0.09
K562-s untreated	1,175.07 ± 64.99	95.47 ± 11.98	2.28 ± 0.33	0.33 ± 0.06
K562-s +1 μmol/L (24 h)	1,019.34 ± 100.61**	77.82 ± 15.41*	1.32 ± 0.25***	0.19 ± 0.07*
K562-r (1 μmol/L)	1,459.78 ± 120.89***	138.04 ± 33.68**	2.14 ± 0.79	0.26 ± 0.01

NOTE: Results are given as mean ± SD ($n = 6$ for each group). Significance levels (*, $P < 0.05$; **, $P < 0.01$; ***, $P < 0.001$) were determined by ANOVA (with post hoc pairwise multiple comparison Tukey test).

ferent. The localization of GLUT-1 is no longer uniform and much of the staining occurs in globular punctate structures. Additionally, much of the staining is no longer associated with the plasma membrane, indicating that GLUT-1 is relocalized in these cells. Finally, in imatinib-resistant K562-r cells, GLUT-1 localization is similar to that of untreated cells in which the transporter is largely associated with the plasma membrane and the staining pattern is much more uniform. These experiments were repeated using the corresponding LAMA84 cell lines with similar outcomes (data not shown). Our results indicate that the differences in glucose uptake and utilization of imatinib-sensitive cells treated with imatinib are, at least in part, due to alterations in the localization of the GLUT-1 glucose transporter.

We next wanted to determine if changes in protein expression play a role in these processes as well. As shown in Fig. 5B, we found no significant differences in GLUT-1 protein levels in either K562 or LAMA84 cells, regardless of imatinib sensitivity. No changes were observed either in GLUT-1 mRNA levels as determined by reverse transcription-PCR (data not shown). These results suggest that changes in glucose uptake cannot be attributed to alterations in GLUT-1 protein levels, but rather to its translocation in the cytosol, which happens even in the first 24 hours of treatment.

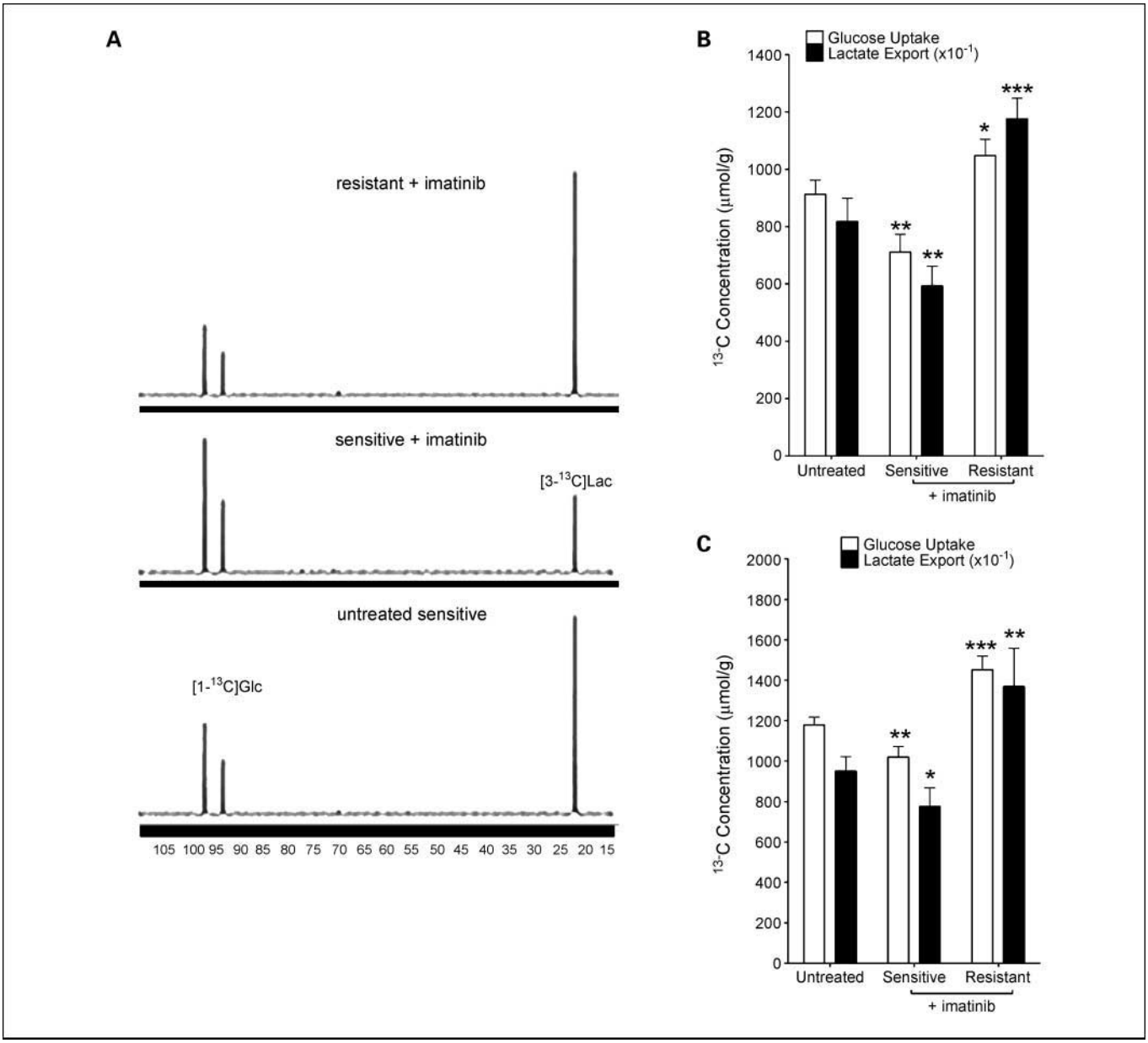

Fig. 2. Representative ^{13}C-MRS on cell media of K562 cells (*A*), as well as [1-^{13}C]glucose uptake and [3-^{13}C]lactate export in LAMA84 (*B*) and K562 (*C*) cells as calculated from ^{13}C-MRS. For glucose and lactate concentrations ($n = 6$ repeats in each group) statistical significance was calculated using Student's *t* test (*, $P < 0.05$; **, $P < 0.01$; ***, $P < 0.001$).

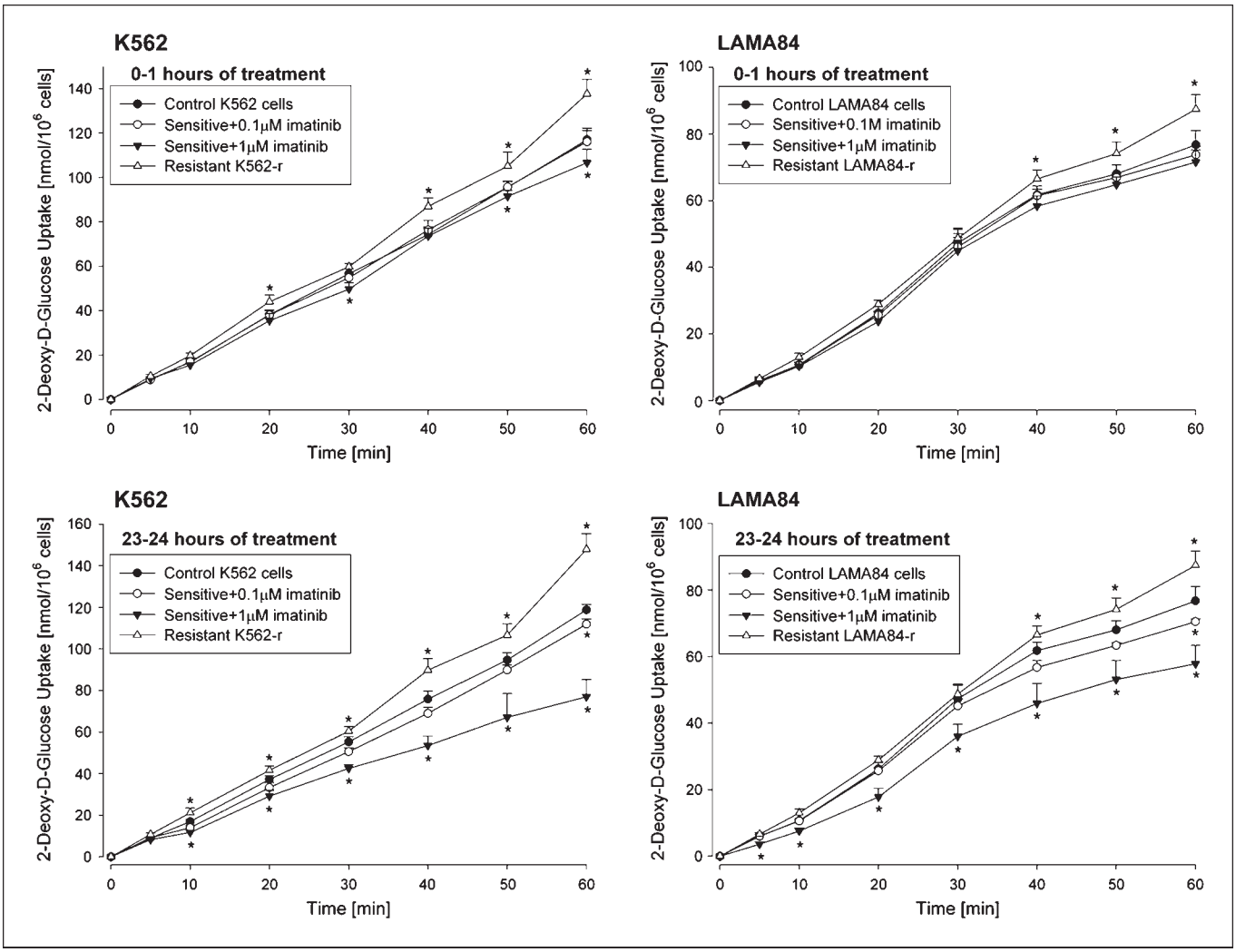

Fig. 3. 2-Deoxy-[1-^{3}H]glucose uptake in imatinib-sensitive and imatinib-resistant K562 and LAMA84 cells. The sensitive cells were treated with 0.1 or 1 μmol/L of imatinib for 1 and 24 h; resistant cells were kept constantly in the presence of 1 μmol/L of imatinib. The cells were incubated with 2-deoxy-[1-^{3}H] glucose for the indicated time periods. The intracellular concentrations of 2-deoxy-[1-^{3}H]glucose were reported as nmol/10^6 cells. All experiments were repeated four times. Points, mean; bars, SD (*, $P < 0.05$ significance level for all tests).

Discussion

Despite its highly specific mechanism of action, the development of primary and secondary resistance to imatinib treatment occurs in patients. Primary resistance to imatinib, defined as an inability to achieve landmark response, is comprised of the 2% of patients who fail to achieve hematologic response and 8% to 13% who fail to achieve major or complete cytogenetic response initially (30). Up to 80% of CML patients in blast phase will relapse while on imatinib after 24 months of treatment. Strictly defining patients with secondary resistance—those who achieve but subsequently lose relevant response—is most straightforward for overt relapse such as loss of cytogenetic or hematologic response and progression from chronic to advanced-stage disease (30, 31). The first challenge is to identify patients who are going to develop imatinib resistance early, and the second is to initiate combination therapies to overcome acquired resistance. Therefore, reliable markers that can predict the early development of resistance to imatinib are in demand. In the present study, we showed that decreased glucose uptake due to (*a*) decreased glycolysis, (*b*) decreased RNA synthesis via the nonoxidative transketolase pathway, and (*c*) intracellular GLUT-1 translocalization are hallmarks of imatinib responsiveness in CML cells even after 24 hours of treatment.

The utilization of glucose is central to all metabolism. It is the universal fuel for human cells for energy production and the carbon source for the synthesis of major endogenous compounds such as lipids, proteins, amino acids, and nucleic acids. Since Warburg's discovery of abnormally elevated "aerobic" glycolysis in the cancer cell (32), a great deal of research has provided additional information and evidence on mitochondrial metabolic dysfunctions and highly elevated glycolysis in cancer cells. Due to the low metabolic state of the cancer cell, as defined by a bioenergetic mitochondrial index relative to the cellular glycolytic potential, glucose uptake in the cancer cell is abnormally high and provides a signature of carcinogenesis (33). Cancer cells often up-regulate the rate-limiting processes and enzymes of glycolysis, including glucose transporters, for instance as a result of the expression of oncogenes including *RAS*, *SRC*, or *BCL-ABL* (34–36). Similarly, activation of the

oncogenic serine/threonine kinase AKT is commonly observed in cancer cells (34) and is also an important downstream effector of numerous oncogenes, including *HER2/neu*, *RAS*, and *BCR-ABL*. Indeed, in our study, *BCR-ABL*–positive cells showed highly elevated glucose uptake and lactate production as well as lactate export into the medium (Figs. 2 and 3). At its therapeutically relevant concentrations, imatinib decreases glucose uptake by translocalization of GLUT-1 transporters from the cell membrane into the cytosol, and by inhibiting glycolysis and promoting mitochondrial oxidative glucose utilization occurring through a cytostatic mechanism of action in the absence of apoptosis or necrosis. Thus, rapid decrease of 18-fluoro-2-deoxy-D-glucose (FDG) uptake on clinical positron emission tomography scans, previously observed only after 24 hours of imatinib treatment in patients with gastrointestinal stromal tumors (22), when tumor burden cannot possibly be reduced, may be partly explained by GLUT-1 translocation in KIT-positive cancer cells.

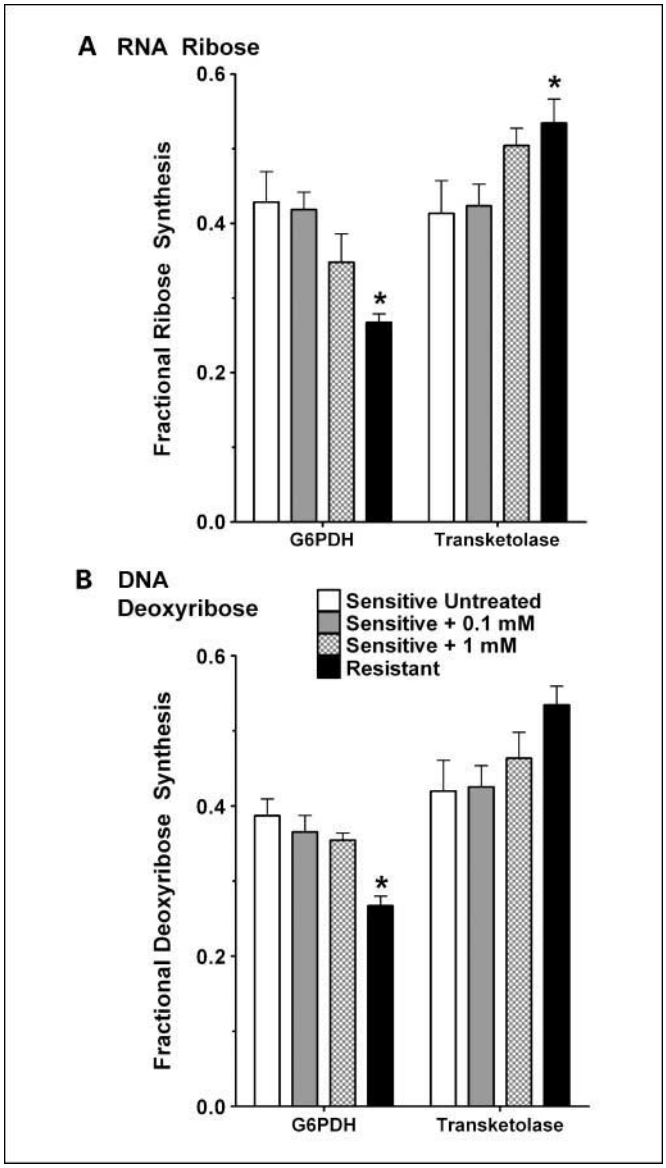

Fig. 4. Results of GC-MS profiling on glucose fluxes in imatinib-treated and resistant cell lines. For the GC-MS analysis of nucleic acid synthesis, cells were incubated with imatinib at the indicated concentrations and at 5 mmol/L [1,2-^{13}C]glucose for 60 h. Columns, fractional synthesis of ribose (*A*) and deoxyribose (*B*) through the oxidative pathway via G6PDH or the nonoxidative glucose pathway via transketolase activity. All experiments were repeated four times (*, $P < 0.05$, significance level for all tests). The representative carbon fluxes from [1,2-^{13}C]glucose through the oxidative branch of the pentose cycle, [1-^{13}C]ribose and [1-^{13}C]deoxyribose, and through the nonoxidative branch, [1,2-^{13}C]ribose and [1,2-^{13}C]deoxyribose, are presented in Fig. 1.

BCR-ABL–positive imatinib-resistant cells, on the other hand, showed an up-regulated glucose uptake, caused by increased glycolytic and low mitochondrial activity, which are among the most important hallmarks of oncogenesis (37, 38). The localization of GLUT-1 transporters in the membrane surface was not significantly different from that of their sensitive untreated counterparts. Additionally, imatinib-resistant cells showed decreased oxidative synthesis of RNA ribose via G6PDH and increased glucose flux to RNA synthesis via the nonoxidative transketolase pathway.

Recently, it has been shown that inhibition of the upstream signal transduction pathway using mammalian target of rapamycin (mTOR) inhibitors can inhibit the proliferation of *BCR-ABL*–positive cells, and thus, be alternative therapies for patients with imatinib-resistant CML (39). Previously, we have shown that the mammalian target of rapamycin inhibitors sirolimus and its derivative everolimus (RAD001), are potent inhibitors of glycolysis in brain cancer cells as well as in healthy astrocytes (40). Additionally, it has been shown that in human lymphocytes, sirolimus inhibits aldolase A, a key glycolytic enzyme (41). Therefore, inhibition of the upstream mTOR pathway in imatinib-resistant cells may lead to the same metabolic phenotype that is characteristic of sensitive cells following the inhibition of BCR-ABL kinase activity.

^{13}C-magnetic resonance spectroscopy (MRS), which assesses not only glucose uptake, but also the metabolism of nonradioactive ^{13}C-labeled tracers, may present a useful alternative to positron emission tomography for patients with CML. For patients with leukemia, a ^{13}C-MRS–based approach will allow for the precise assessment of glucose uptake and metabolism (glycolysis and the Krebs cycle) in isolated leukocytes after incubation with ^{13}C-labeled glucose. Simultaneously, quantification of other important carbon fluxes in the same sample can be done with the GC-MS approach. The combination of these two techniques allows precise monitoring of diverse changes in metabolic fluxes occurring in cells: from cytosol to mitochondria, and from glycolysis to fatty acids, RNA, and DNA synthesis.

The metabolic signature of imatinib resistance—i.e., increased glucose consumption and glycolytic activity accompanied by relatively high GLUT-1 expression on the cell surface—can reliably reveal therapeutic sensitivity to imatinib treatment. This can be readily evaluated by MRS in CML cell lines as well as applied to assess glucose metabolism in leukocytes isolated from patients with imatinib-treated CML, using the same approach as described in the present study with clonal cell lines. In future clinical studies, we will test whether the metabolic effect [increased glucose uptake with elevated (glycolysis/TCA) ratios] can be detected in the "to-be-resistant" cells prior to an increase in the white cell count. Indeed, increased accumulation of FDG in positron emission tomography studies (indicating increased GLUT-1 and hexokinase activity) often appears before anatomically visible tumor growth in therapy-resistant solid tumors (42). If validated, the glucose assessment

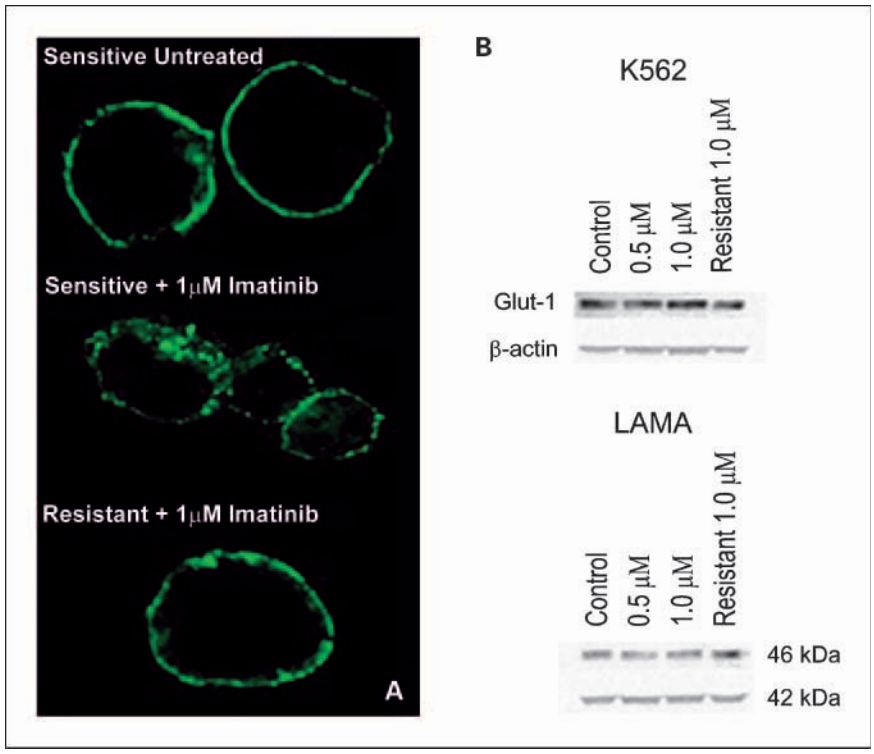

Fig. 5. *A,* microscopy of GLUT-1 protein localization in K562 cells treated for 24 h with 1 μmol/L of imatinib. Results are representative of three separate experiments. *B,* Western blot of K562 and LAMA84 cells harvested after 24 h of treatment with imatinib at the indicated concentrations and probed with anti–Glut-1 and anti-actin antibodies. Results are representative of three separate experiments.

can help to (*a*) develop a clinical MRS-based metabolic profile in peripheral blood (equivalent to positron emission tomography studies in solid tumors) for the early detection of imatinib resistance in patients with CML, and (*b*) to evaluate the metabolic mechanisms of action for novel small molecule tyrosine kinase inhibitors. In addition, targeted therapies, which include metabolic enzyme inhibitors (such as glycolytic or transketolase inhibitors), may be tested as possible therapeutic alternatives for imatinib-resistant cells.

Disclosure of Potential Conflicts of Interest

No potential conflicts of interest were disclosed.

Acknowledgments

We thank Dr. Elisabeth Buchdunger (Novartis Pharma AG) for imatinib supply and helpful discussions.

References

1. Nowell PC, Hungerford DA. Chromosome studies on normal and leukemic human leukocytes. J Natl Cancer Inst 1960;25:85–109.
2. Rowley JD. Letter: A new consistent chromosomal abnormality in chronic myelogenous leukaemia identified by quinacrine fluorescence and Giemsa staining. Nature 1973;243:290–3.
3. Heisterkamp N, Stephenson JR, Groffen J, et al. Localization of the c-ab1 oncogene adjacent to a translocation break point in chronic myelocytic leukaemia. Nature 1983;306:239–42.
4. Buchdunger E, Zimmermann J, Mett H, et al. Inhibition of the Abl protein-tyrosine kinase *in vitro* and *in vivo* by a 2-phenylaminopyrimidine derivative. Cancer Res 1996;56:100–4.
5. Druker BJ, Tamura S, Buchdunger E, et al. Effects of a selective inhibitor of the Abl tyrosine kinase on the growth of Bcr-Abl positive cells. Nat Med 1996;2:561–6.
6. Kantarjian HM, Talpaz M, Giles F, O'Brien S, Cortes J. New insights into the pathophysiology of chronic myeloid leukemia and imatinib resistance. Ann Intern Med 2006;145:913–23.
7. Talpaz M, Shah NP, Kantarjian H, et al. Dasatinib in imatinib-resistant Philadelphia chromosome-positive leukemias. N Engl J Med 2006; 354:2531–41.
8. Druker BJ. Circumventing resistance to kinase-inhibitor therapy. N Engl J Med 2006; 354:2594–6.
9. Assef Y, Rubio F, Colo G, Del Monaco S, Costas MA, Kotsias BA. Imatinib resistance in multidrug-resistant K562 human leukemic cells. Leuk Res 2009;33:710–6.
10. Donato NJ, Wu JY, Stapley J, et al. BCR-ABL independence and LYN kinase overexpression in chronic myelogenous leukemia cells selected for resistance to STI571. Blood 2003;101:690–8.
11. Gorre ME, Mohammed M, Ellwood K, et al. Clinical resistance to STI-571 cancer therapy caused by BCR-ABL gene mutation or amplification. Science 2001;293:876–80.
12. Hochhaus A, Kreil S, Corbin AS, et al. Molecular and chromosomal mechanisms of resistance to imatinib (STI571) therapy. Leukemia 2002;16: 2190–6.
13. Jiang X, Saw KM, Eaves A, Eaves C. Instability of BCR-ABL gene in primary and cultured chronic myeloid leukemia stem cells. J Natl Cancer Inst 2007;99:680–93.
14. Roche-Lestienne C, Soenen-Cornu V, Grardel-Duflos N, et al. Several types of mutations of the Abl gene can be found in chronic myeloid leukemia patients resistant to STI571, and they can pre-exist to the onset of treatment. Blood 2002; 100:1014–8.
15. White DL, Saunders VA, Dang P, et al. OCT-1-mediated influx is a key determinant of the intracellular uptake of imatinib but not nilotinib (AMN107): reduced OCT-1 activity is the cause of low *in vitro* sensitivity to imatinib. Blood 2006;108:697–704.
16. Boros LG, Cascante M, Lee WN. Metabolic profiling of cell growth and death in cancer: applications in drug discovery. Drug Discov Today 2002;7:364–72.
17. Serkova N, Boros LG. Detection of resistance to imatinib by metabolic profiling: clinical and drug development implications. Am J Pharmacogenomics 2005;5:293–302.
18. Gottschalk S, Anderson N, Hainz C, Eckhardt SG, Serkova NJ. Imatinib (STI571)-mediated changes in glucose metabolism in human leukemia BCR-ABL-positive cells. Clin Cancer Res 2004;10:6661–8.
19. Boren J, Cascante M, Marin S, et al. Gleevec (STI571) influences metabolic enzyme activities and glucose carbon flow toward nucleic acid and fatty acid synthesis in myeloid tumor cells. J Biol Chem 2001;276:37747–53.
20. Boros LG, Lee WN, Cascante M. Imatinib and

chronic-phase leukemias. N Engl J Med 2002; 347:67–8.

21. Barnes K, McIntosh E, Whetton AD, Daley GQ, Bentley J, Baldwin SA. Chronic myeloid leukaemia: an investigation into the role of Bcr-Abl-induced abnormalities in glucose transport regulation. Oncogene 2005;24:3257–67.

22. Hughes B, Yip D, Goldstein D, Waring P, Beshay V, Chong G. Cerebral relapse of metastatic gastrointestinal stromal tumor during treatment with imatinib mesylate: case report. BMC Cancer 2004;4:74.

23. Van den Abbeele AD, Badawi RD. Use of positron emission tomography in oncology and its potential role to assess response to imatinib mesylate therapy in gastrointestinal stromal tumors (GISTs). Eur J Cancer 2002;38, Suppl 5:S60–5.

24. Breccia M, Muscaritoli M, Aversa Z, Mandelli F, Alimena G. Imatinib mesylate may improve fasting blood glucose in diabetic Ph+ chronic myelogenous leukemia patients responsive to treatment. J Clin Oncol 2004;22:4653–5.

25. Breccia M, Muscaritoli M, Cannella L, Stefanizzi C, Frustaci A, Alimena G. Fasting glucose improvement under dasatinib treatment in an accelerated phase chronic myeloid leukemia patient unresponsive to imatinib and nilotinib. Leuk Res 2008;32:1626–8.

26. Mahon FX, Deininger MW, Schultheis B, et al. Selection and characterization of BCR-ABL positive cell lines with differential sensitivity to the tyrosine kinase inhibitor STI571: diverse mechanisms of resistance. Blood 2000;96:1070–9.

27. Pfaffl MW. A new mathematical model for relative quantification in real-time RT-PCR. Nucleic Acids Res 2001;29:e45.

28. Maraldi T, Fiorentini D, Prata C, Landi L, Hakim G. Glucose-transport regulation in leukemic cells: how can H_2O_2 mimic stem cell factor effects? Antioxid Redox Signal 2007;9:271–9.

29. Boros LG, Williams RD. Isofenphos induced metabolic changes in K562 myeloid blast cells. Leuk Res 2001;25:883–90.

30. Hochhaus A, Druker B, Sawyers C, et al. Favorable long-term follow-up results over 6 years for response, survival, and safety with imatinib mesylate therapy in chronic-phase chronic myeloid leukemia after failure of interferon-α treatment. Blood 2008;111:1039–43.

31. Zeidan A, Wang ES, Wetzler M. What Is imatinib-resistant chronic myeloid leukemia? Identifying and managing loss of response. Clin Adv Hematol Oncol 2008;6:673–83.

32. Warburg O. On the origin of cancer cells. Science 1956;123:309–14.

33. Kroemer G. Mitochondria in cancer. Oncogene 2006;25:4630–2.

34. Elstrom RL, Bauer DE, Buzzai M, et al. Akt stimulates aerobic glycolysis in cancer cells. Cancer Res 2004;64:3892–9.

35. Pelicano H, Martin DS, Xu RH, Huang P. Glycolysis inhibition for anticancer treatment. Oncogene 2006;25:4633–46.

36. Pelicano H, Xu RH, Du M, et al. Mitochondrial respiration defects in cancer cells cause activation of Akt survival pathway through a redox-mediated mechanism. J Cell Biol 2006;175:913–23.

37. Lyon RC, Cohen JS, Faustino PJ, Megnin F, Myers CE. Glucose metabolism in drug-sensitive and drug-resistant human breast cancer cells monitored by magnetic resonance spectroscopy. Cancer Res 1988;48:870–7.

38. Zhou R, Vander Heiden MG, Rudin CM. Genotoxic exposure is associated with alterations in glucose uptake and metabolism. Cancer Res 2002;62:3515–20.

39. Kharas MG, Janes MR, Scarfone VM, et al. Ablation of PI3K blocks BCR-ABL leukemogenesis in mice, and a dual PI3K/mTOR inhibitor prevents expansion of human BCR-ABL+ leukemia cells. J Clin Invest 2008;118:3038–50.

40. Serkova N, Jacobsen W, Niemann CU, et al. Sirolimus, but not the structurally related RAD (everolimus), enhances the negative effects of cyclosporine on mitochondrial metabolism in the rat brain. Br J Pharmacol 2001;133:875–85.

41. Wang X, Luo H, Perks A, Wu J. Rapamycin inhibits aldolase A expression during human lymphocyte activation. J Cell Biochem 1996; 63:239–51.

42. Grimpen F, Yip D, McArthur G, et al. Resistance to imatinib, low-grade FDG-avidity on PET, and acquired KIT exon 17 mutation in gastrointestinal stromal tumour. Lancet Oncol 2005; 6:724–7.